Jurnal
Teknologi

Full Paper

EMG RECORDING OF WRIST GESTURES UNDER NON-IDEAL ELECTRODE PLACEMENT FOR MACHINE CONTROL IN A MANUFACTURING ENVIRONMENT

Zinvi Fu[a*], A. Y. Bani Hashim[a], Z. Jamaludin[a], I. S. Mohamad[b]

[a]Department of Robotics & Automation, Faculty of Manufacturing Engineering, Universiti Teknikal Malaysia Melaka, Melaka, Malaysia.
[b]Department of Thermal Fluid, Faculty of Mechanical Engineering, Universiti Teknikal Melaka Malaysia, 76100 Durian Tunggal, Melaka, Malaysia

*Corresponding author
zinvifu@yahoo.com

Article history
Received
15 May 2015
Received in revised form
12 September 2015
Accepted
30 September 2015

Graphical abstract

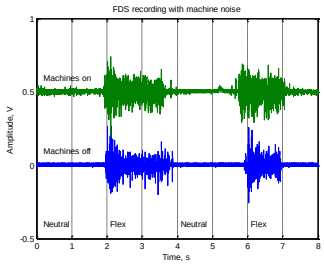

Abstract

The use of electromyography (EMG) for machine control in a manufacturing environment is challenging due to the inherent electrical noise, and also because machine operators lack anatomy knowledge of muscle location for electrode placement. In this research, an electrode placement scheme is proposed for this user group. An EMG preamp was constructed to observe EMG patterns in lower forearm when electrodes placed by untrained operators are in less optimal locations. Crosstalk was found to be a major issue when electrodes are placed in imperfect locations. The EMG preamplifier was deliberately constructed with low cost components to simulate the increased floor noise due to electrical interferences f however from the results, the resulting SNR is acceptable. This study shows that in designing a practical EMG input system, electrode placement is a bigger factor compared to electrical interference.

Keywords: Electromyography, EMG Human Machine Interface, Synthetic System, lower forearm muscles, biosignal data acquisition, manufacturing environment

Abstrak

Penggunaan electromiografi (EMG) untuk kawalan mesin dalam kawasan pembuatan adalah mencabar akibat hingar elektrik, dan juga pengendali mesin tidak mempunyai pengetahuan anatomi mengenai lokasi otot untuk penempatan elektrod. Penguat EMG telah dibina untuk mendapatkan hasil keluaran EMG pada lengan bawah seandainya elektrod diletakkan pada lokasi tidak optima oleh pengendali yang tidak terlatih. Kesan hingar dari mesin adalah minima, tetapi hingar silang antara otot merupakan isu utama ketika elektrod diletakkan pada lokasi yang kurang sempurna. Pembinaan penguat EMG ini disengajakan dengan komponen kos rendah demi mensimulasi hingar lantai yang lebih tinggi akibat gangguan elektrik. Namun, keputusan telah menunjukkan SNR yang masih boleh diterima. Kajian ini telah menunjukkan bahawa perletakan elektrod EMG merupakan factor utama dalam proses membina peranti input EMG yang praktikal.

Kata kunci: Electromiografi, EMG, antaramuka manusia mesin, system sintetik, otot lengan bawah, isyarat bio, manufacturing environment

1.0 INTRODUCTION

The surface EMG (sEMG) has been traditionally used for diagnosis of neuro-muscular conditions [1&2]. Recent researches have shown that sEMG signal also carries information on biometric identification [3] and fatigue [4], besides motion prediction [5]. These features of the sEMG open up the possibility of human-machine integration (HMI), which is one of the enabling technologies in an Intelligent Manufacturing System (IMS) layout. In an IMS, human-machine interaction is two way; humans can learn from machines and vice-versa [6&7].

The benefits of using sEMG in manufacturing are double-edged; sEMG relates directly to the human body movement, thus it is possible to develop highly intuitive machine control interfaces. At the same time, the unique biometric element of the sEMG allows for user identification and instantaneous retrieval of jobs and task specifications. Finally, if the sEMG has been in recording, a computer can access the state of health of an operator and raise alarm if fatigue or unpredictable movement is detected. In a Computer Integrated Manufacturing (CIM) layout, these data can be shared with other devices and users. The effective integration of data can reduce conveyance time and human error, thus reducing downtime and waste.

In our previous work, we have detailed how the sEMG human-machine interface can contribute to the manufacturing environment, and also proposed a practical sEMG electrode placement strategy for the manufacturing operator [8] [9]. Using the sEMG in the manufacturing environment posses its own set of challenges; first, machine operators are not trained to carry out electrode placement and should not be burdened to do so. Unfortunately the sEMG system setup is complicated and the user requires anatomic knowledge of the target muscles, since precise electrode placement is critical [8,10&11]. Secondly the factory environment is electrically noisy and electromagnetic interference (EMI) from power lines, switching devices and motors (CITATION) may corrupt the EMG signals through capacitive coupling to the body, amplification circuit and cables [12].

For machine control, recent experiments show very high classification rate of over 90% (CITATION). However, these results were obtained under optimal conditions in laboratories, i.e. strategic electrode placement and adequate noise suppression [10,13-15]. Serious considerations must take place before industrial implementation. In most cases electrode placement is time consuming and lacks practicality. While a high degree of dimensionality can be achieved with sEMG, a large number of electrodes is required - some over deep muscles [10,16&17]. In practice, the operator does not have ample time and knowledge to place the electrodes and erroneous placements will result readings beyond the feature extraction and classification definition. To date, there are no demonstrations of sEMG machine control in a practical environment, with the exception for [18], which requires up to 30 minutes of calibration per session. Therefore at this juncture, we can conclude that difficulties in sEMG control system lies in the ease of setup, especially in electrode placement.

In this paper, the effects of poorly placed electrodes within an electrically noisy environment are explored. The motivation of the setup is to obtain results of sEMG whereby electrode placement is done by untrained personnel and EMG preamplification is done with minimal noise suppression to simulate a noisy industrial environment. EMG signals from six lower forearm muscles were evaluated, namely the flexor carpi radialis (FCR), flexor carpi ulnaris (FCU), flexor digitorum superficialis (FDS), extensor carpi ulnaris (ECU), extensor carpi radialis (ECR) and extensor digitorum (EDT). Various gestures were performed and the multi channel waveforms were recorded. These muscles are selected because they are close to the elbow and thus not susceptible to displacement during forearm rotation.

2.0 EXPERIMENTAL PROCEDURES

2.1 Electrode Placement Scheme

In order to make the sEMG system viable for everyday uses, it must be practical and the user of the sEMG system should not be burdened with clinical setup. Our approach to the problem is to develop the sEMG system with minimal electrodes. In order to achieve this, we aim to use fewer but significant forearm muscle, while maximizing the number of classifiable gestures.

An electrode grid is presented in Figure 1 (a). Through palpation, the locations of the muscle belly are marked with a coordinate system. The coordinates for six muscles, FCU, FCR, FDS, ECU, ECR and EDT are recorded in Table 1.

Table 1 Results of palpation and muscle coordinates

Muscles not prone to shift during rotation of the forearm	
FDS	(3,6)
FCR	(3,2)
FCU	(2,2)
EDT	(-3,3)
ECRL, ECRB	(-2,1)
ECU	(-4,1)

The gestures that relate to the six muscles, summarized from [19] are shown in Table 2. For instance, the wrist flexion gesture involves the contraction of the FCU, FCR, and FDS. The ECU, ECR and EDT muscles are not contracted for wrist flexion. Written as a logic function, the wrist flexion is defined as $= FCU.FCR.FDS.\overline{ECU}.\overline{ECR}.\overline{EDT}$. The definitions for the other gestures are detailed in Table 2

Table 2 Major muscles and their functions

Gesture	Muscles Involved						Logic function of Gesture
	FCU	FCR	FDS	ECU	ECR	EDT	
Flex, F	1	1	1	0	0	0	$F = FCU.FCR.FDS.\overline{ECU}.\overline{ECR}.\overline{EDT}$
Extend, E	0	0	0	1	1	1	$E = \overline{FCU}.\overline{FCR}.\overline{FDS}.ECU.ECR.EDT$
Radial deviation, RD	0	1	0	0	1	0	$AB = \overline{FCU}.FCR.\overline{FDS}.\overline{ECU}.ECR.\overline{EDT}$
Ulnar deviation, UD	1	0	0	1	0	0	$AD = FCU.\overline{FCR}.\overline{FDS}.ECU.\overline{ECR}.\overline{EDT}$
Hand open, HO	0	0	1	0	0	0	$HO = \overline{FCU}.\overline{FCR}.FDS.\overline{ECU}.\overline{ECR}.\overline{EDT}$
Hand Close, HC	0	0	0	0	0	1	$HC = \overline{FCU}.\overline{FCR}.\overline{FDS}.\overline{ECU}.\overline{ECR}.EDT$

We propose the grid system to be implemented onto a flexible material that would be constructed in the form of a wearable sleeve. This sleeve would stretch with the skin as the forearm rotates (Figure (b)).

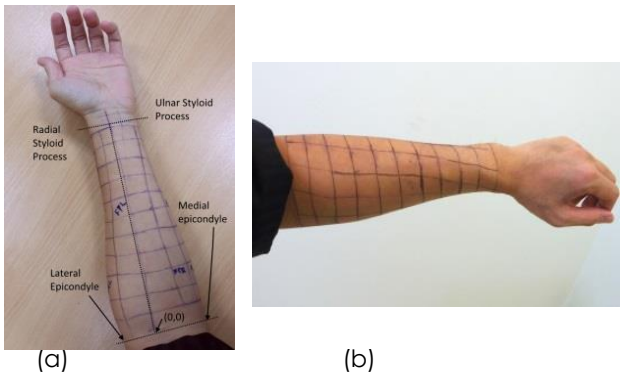

(a) (b)

Figure 1 Coordinate system for locating muscles in the forearm

Together with the coordinate system, we also defined the gestures of the wrist and hand muscles as logical functions based on the functions in Table 2.

2.2 Channel mapping

The muscles of the forearm are mapped according to the setup in Table 2. The electrodes that were used are pre-gelled disposable Ag-Cl type. Two electrodes per channel with a spacing of 3cm were placed over each of the muscles. Crocodile clips were used to connect the electrode to the preamplifier inputs.

Table 3 Channel mapping of the experimental setup

Channel	CH1	CH2	CH3	CH4	CH5	CH6
Muscle	EDT	FDS	ECR	FCR	ECU	FCU

Skin preparation was also performed to provide better electrical contact. The skin was shaved and swabbed with alcohol prior to electrode adhesion.

2.3 Design of Experiment

For this experiment, a six-channel EMG amplifier was constructed. Six pairs of Ag-Cl wet electrodes were used to acquire the EMG signals produced by the six muscles. The output of each channels were fed into a digital storage oscilloscope (DSO) and recorded into CSV files. These CSV files were later reconstructed with Matlab. The design of the circuitry is based on [20]. The experimental setup is shown in Figure 2(a). In Figure 2(b), the EMG waveform for wrist flexion over the FDS can be observed in the oscilloscope.

With this configuration, CH1 served as a reference while CH2-CH6 represents EMG recording in an electrically noisy environment with minimal noise reduction.

(a) (b)

Figure 2 Experiment setup for EMG

2.3 Recording Environment

To observe the effect of noise due to equipment, the EMG recording was done in proximity to various manufacturing equipments as seen in Figure 3. The procedure was repeated when the machines were running and when they were off.

2.4 Circuit Design Of The EMG Amplifier

A classic bipotential instrumentation amplifier configuration is used here. In normal circumstances, much attention would be paid to noise reduction. However, this simplistic implementation was deliberated; noise rejection is reduced to just common grounding and bandpass filtering. In addition, the preamplifier circuits were constructed with low cost discrete op-amps. The circuit was constructed on a breadboard with no shielding. The reason for this atypical setup is to allow EMI capacitive coupling from nearby machines to interfere with the EMG acquisition. Two versions of the amplifiers were constructed. Channel 1 (CH1) was built with using an intergrated instrumentation amplifier IC while Channel 2-6 (CH2-CH6) were built with discrete op-amps.

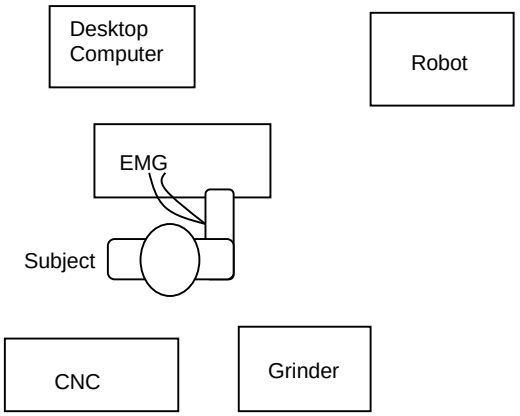

Figure 3 Environment of experimental setup

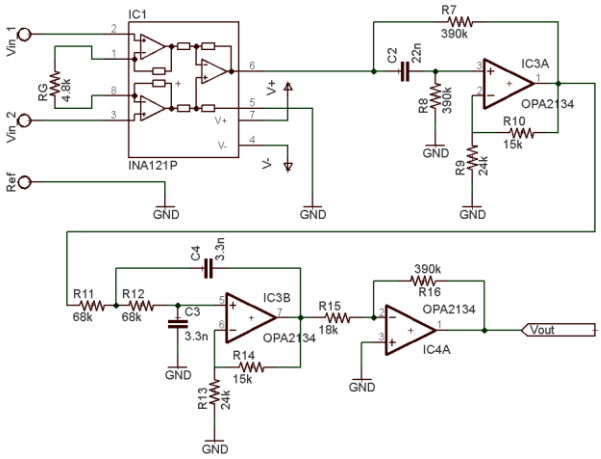

Figure 4 Schematics for CH1

2.5 The Preamplifier Stage

Instrumentation amplifiers (INA) consisting of a buffer stage and differential amplifier, are available as a single package or alternatively can be built with discreet op-amps. Many literatures recommend INAs over standard op-amps for EMG amplification circuits [18,20-22], because resistor mismatch causes imbalanced gain in between the inverting and non-inverting channels which compromises the CMRR at the differential stage.

Figure 4 illustrates the circuit for CH1. The INA121P by Texas Instruments has a CMRR of 100 and bandwidth of 600kHz, it's specification is sufficient for our application for low frequency signals. For CH2-CH6, the internal circuit of the INA121P was replicated with the JRC4558 op-amp and 1% resistors. Note that other than the components in the preamplifier, the rest of the circuit is similar to that of CH1. A gain of 10x was applied because at this level, the CMRR of the INA121P was near maximum of 100dB. Further increasing the gain would reduce the bandwidth and introduce noise.

For CH2-CH6, shown in Figure 5the internal circuit of the INA121P was replicated with the JRC4558 op-amp and 1% resistors. Note that other than the components in the preamplifier, the rest of the circuit is similar to that of CH1. A gain of 10x was applied because at this level, the CMRR of the INA121P was near maximum of 100dB. Further increasing the gain would reduce the bandwidth and introduce noise.

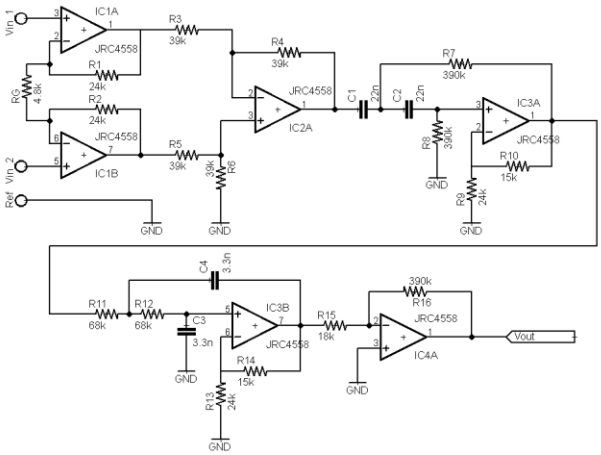

Figure 5 Schematics for CH2-CH6

2.6 The Filter Stage

It is widely accepted that the energetic distribution of the EMG signal is in the range of 20-500Hz [2,20,23&24]. In this research, a second order Sallen-Key active filter topology was used. The filter stages include a low pass (LPF and high pass filter (HPF). The notch filter, commonly used to filter the 50/60Hz power line noise was omitted, because a majority of EMG energy exists near that frequency.

Basing on the resistor and capacitor values in the schematics, the corner frequency, passband gain and Q factor for the filter stage are computed in Table 4.

Table 4 Filter design parameters

	HPF	LPF
Corner frequency, f_c	18.97Hz	709Hz
Passband gain, K	1.625	1.625
Q factor, Q	0.727	0.727

The gain value was set as such to obtain a Q factor in between 0.7 to 1.0 in order to achieve the steepest rolloff possible.

In the circuit, the op-amp used for CH1 is OPA2134 while CH-2-CH6 used JRC4558. OPA2134 is an audio grade op-amp significantly superior compared to the JRC4558 in terms of noise, distortion, CMRR and bandwidth. The frequency response of the individual filter stages can be observed in Figure 6.

2.7 Final Amplification Stage

A final inverting amplification (IVA) stage was used to amplify the signal to a level within the range of the oscilloscope. In order to avoid saturation, the gain was set to a moderate level of 21.67.

The EMG amplifier contains amplification at multiple stages where the total gain is applied is 650. With this level of gain, the signal level is high enough to be acquired by the oscilloscope. Figure 7 shows the overall gain of the circuit across the stages.

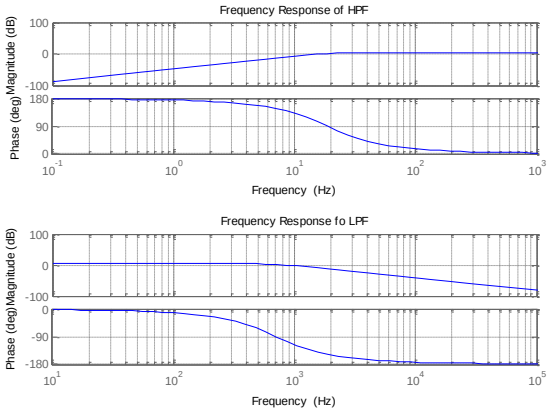

Figure 6 Frequency response plot of the filter stage

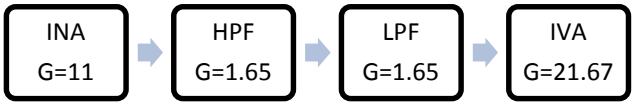

Figure 7 Overall gain of circuit

3.0 RESULTS AND DISCUSSION

3.1 Effects Of Machine Noise To Signal Noise

The results of machine noise to the EMG signal during wrist flexion are shown in Figure 8. During machine operation, some power spikes can be observed in the baseline noise. The noise was extracted and its frequency response is shown in Figure 9. While the dominant noise signal is caused by the 50Hz power line, the machine operation caused a general increase in noise across the spectrum. Our results show that the overall noise increase is negligible. The Signal to noise ratio for both states are shown in Table 5.

Table 1 SNR of EMG signals under test conditions

Machine state	SNR (dB)	Circuit Type	SNR (dB)
Machine On	14.97	INA121P	21.73
Machine Off	15.61	JRC4558	19.79

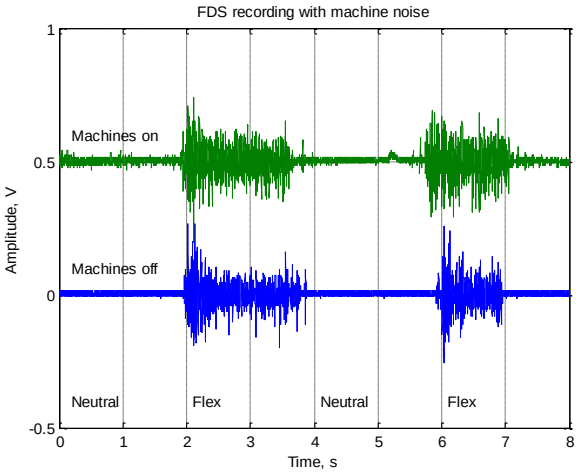

Figure 8 EMG recording during machine operation

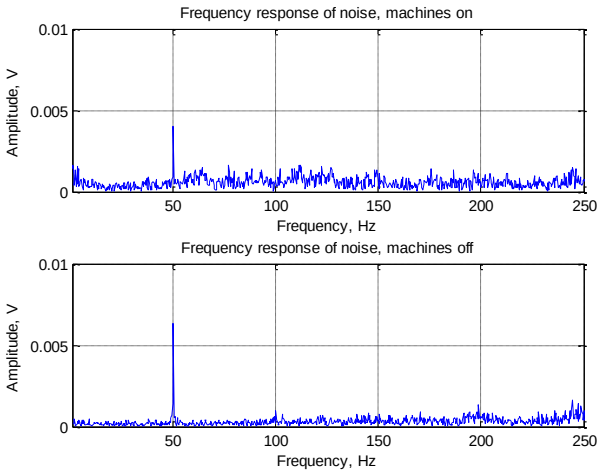

Figure 9 Frequency response of noise

3.2 Performance Comparison Between CH1 And CH2-CH6

The first set of data in Figure 10 shows the EMG waveform taken over CH1 and CH2. CH1 did not show significant advantage of SNR over CH2, despite the integrated INA and high grade op-amps used in CH1. The SNR of the waveform in Figure 8 is shown in Table 5. The SNR of the integrated INA is only slightly higher than the JRC4558.

3.2 Results Of Semg Acquisition

For the experiment, six gestures were performed and the waveform of the corresponding muscles was obtained. The result was compared to the functions defined in Table 1. In Figure 11, the recording was taken when the wrist is in a relaxed, neutral (no wrist rotation) position. A baseline noise can be observed almost uniform across all channels.

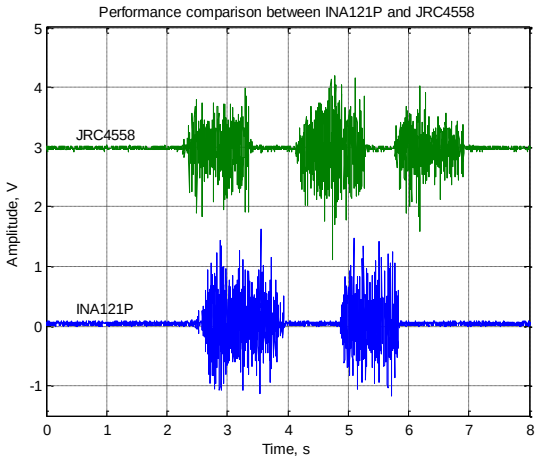

Figure 10 Waveform of wrist extension in CH1 and CH2

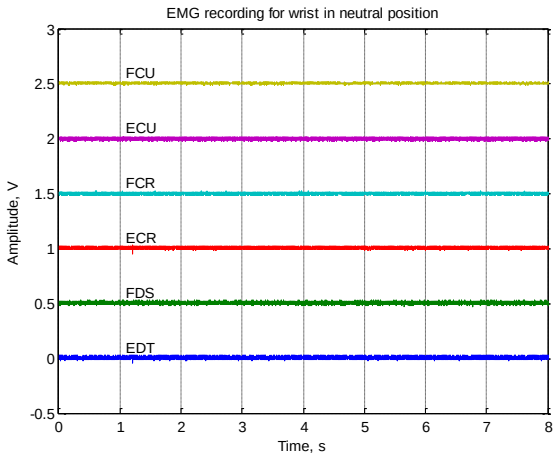

Figure 11 Waveform of EMG signals when wrist is neutral

3.2 Results Of Semg Acquisition

For the experiment, six gestures were performed and the waveform of the corresponding muscles was obtained. The result was compared to the functions defined in Table 1. In Figure 11, the recording was taken when the wrist is in a relaxed, neutral (no wrist rotation) position. A baseline noise can be observed almost uniform across all channels.

During the wrist flexion, the wrist was flexed in normal position. The waveform of the wrist flexion is shown in Figure 12. From the wrist function in Table 2, we expected dominant muscle activities in the flexor muscles. However, this theory was not fully met since dominant muscle activities emerge from the FCU and ECU. For flexion, we expected the FDS to be dominant over the other channels, but this was not the case. The other flexor muscles, FDS and FCR register signs of contraction; however their levels cannot be considered dominant. Some muscle activities were also recorded in the ECR, and EDT channels, which were not expected. A summary of gesture analysis is shown in Table.

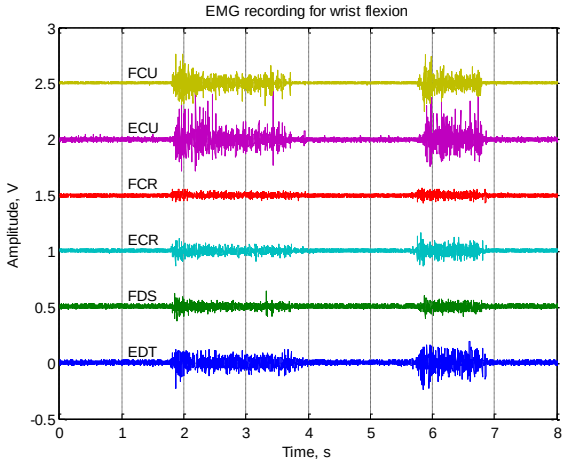

Figure 12 Waveform of EMG signals during wrist flexion

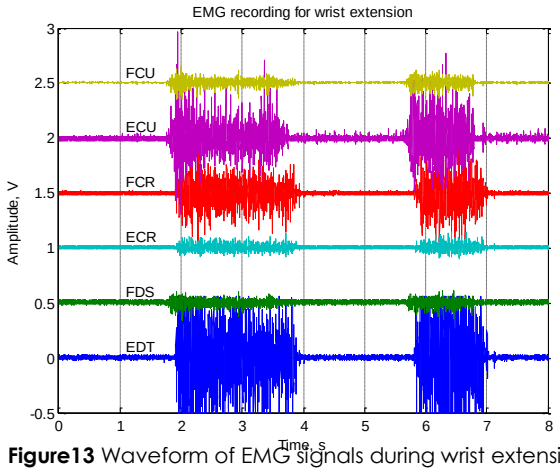

Figure13 Waveform of EMG signals during wrist extension

For the wrist extension shown in Figure 13, the EDT shows a significantly higher level of muscle activity, followed by that of the ECU. The ECR did not how much muscle activity. Other than the FCR, the other flexor muscles show little muscle EMG. The analysis is shown in Table 6 and the decoding algorithm can be partially fulfilled. Close inspection unto the non dominant channels reveal a similar waveform to the dominant channels. This suggests an occurrence of channel crosstalk.

In Figure 14, the EMG recording shows the muscle activity for the ulnar deviation. The ECU registered the highest level of EMG signals followed by the FCU. This is expected as these two muscles are responsible for the ulnar deviation. However, there is also a significant detection of muscle activity from the EDT. At this level, crosstalk is ruled out. The unexpected signal from the

EDT suggests that there may have been some EDT contraction during the ulnar deviation. This may also been caused by improper electrode placement which caused the EDT channel to pick up muscle activity from other muscles.

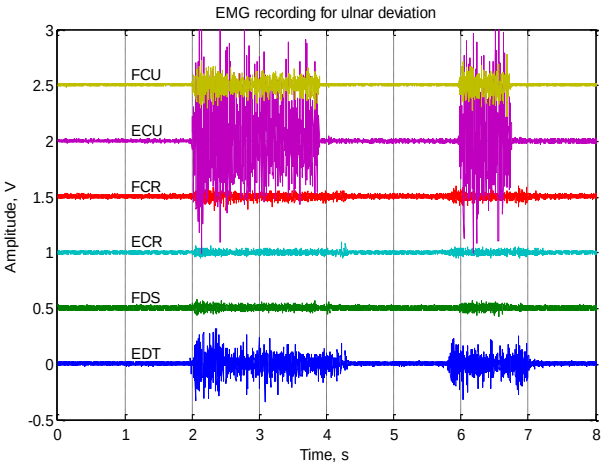

Figure 14 Waveform of EMG signals ulnar deviation

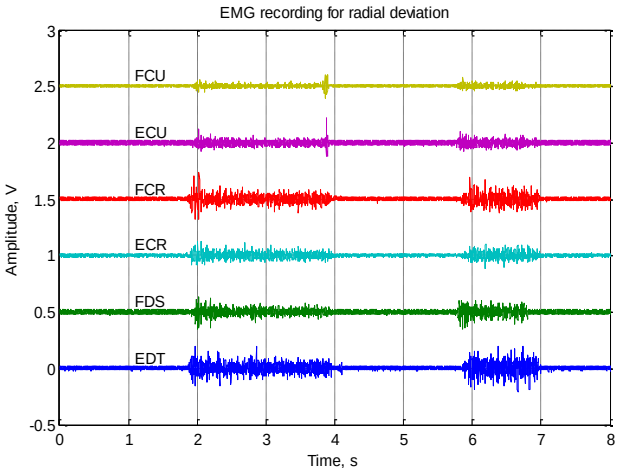

Figure 15 Waveform of EMG signals during wrist radial deviation

For radial deviation (Figure 15), muscle activity was recorded across all channels. The radials muscles did not register significantly higher muscle activities. The uniform waveform across the channels suggest a high level of crosstalk.

In Figure 16 and 17, the waveform of the EMG signal during hand open and hand closed is presented. The EDT channel shows a significant level of muscle activity, and it is dominant over all other channels. Thus, the anatomic logic can be fulfilled. The system also registered muscle activities in all the other muscles. Although the action of opening the fingers is generally accepted as the sole function of the EDT [19,25], in practice however, all the wrist muscles need to be contracted in order to hold the hand in equilibrum force, as one would tend to keep the wrist rigid when having the hand fully open or closed.

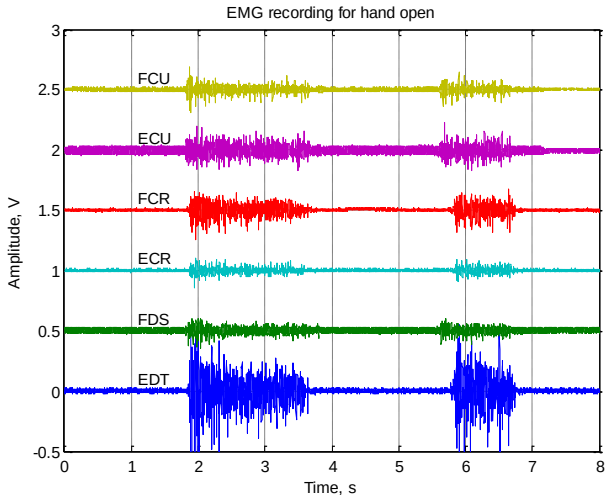

Figrue16 Waveform of EMG signals during hand open

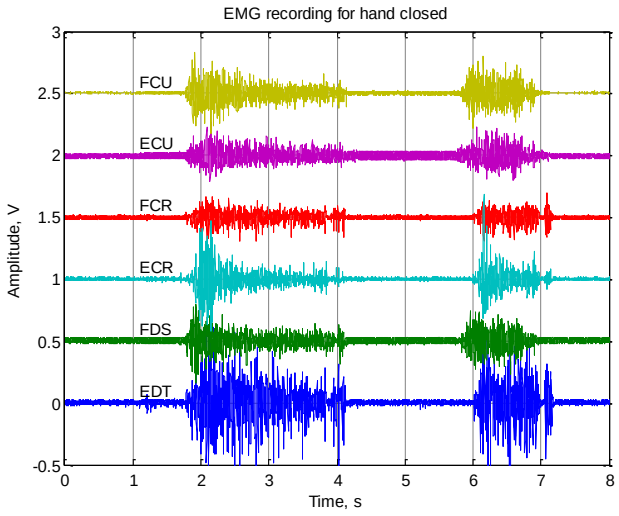

Figure 17 Waveform of EMG signals during hand closed

To understand the muscle activity during hand open and hand close, one must account for the forces acting upon the hand in such gestures. Figure 18 illustrates the forces acting unto the hand when it is held static open or closed. In order to hold the hand static, the flexion, extension and deviation forces must be equal and also overcome the weight of the hand. Equation 1 summarizes the relationship of the forces.

$$F_{nett} = F_{flex} + F_{extend} + F_{ulnar} + F_{radial} + W_{hand} = 0 \quad (1)$$

Table 6 Summary of analysis of EMG waveforms

		Muscles involved							
	Results*	FCU	FCR	FDS	ECU	ECR	EDT	Anatomy logic function	Logic fulfilled
Flex, F	Exp	1	1	1	0	0	0	$F = FCU.FCR.FDS.\overline{ECU}.\overline{ECR}.\overline{EDT}$	No
	Act	*1*	*0*	*0*	*1*	*0*	*0*		
Extend, E	Exp	0	0	0	1	1	1	$E = \overline{FCU}.\overline{FCR}.\overline{FDS}.ECU.ECR.EDT$	Partial
	Act	*0*	*1*	*0*	*1*	*0*	*1*		
Radial Dev, RD	Exp	0	1	0	0	1	0	$AB = \overline{FCU}.FCR.\overline{FDS}.\overline{ECU}.ECR.\overline{EDT}$	No
	Act	*0*	*0*	*0*	*0*	*0*	*0*		
Ulnar Dev, UD	Exp	1	0	0	1	0	0	$AD = FCU.\overline{FCR}.\overline{FDS}.ECU.\overline{ECR}.\overline{EDT}$	Yes
	Act	*0*	*0*	*0*	*1*	*1*	*0*		
Hand open, HO	Exp	0	0	1	0	0	0	$HO = \overline{FCU}.\overline{FCR}.FDS.\overline{ECU}.\overline{ECR}.\overline{EDT}$	No
	Act	*0*	*0*	*0*	*0*	*0*	*1*		
Hand Close, HC	Exp	0	0	0	0	0	1	$HC = \overline{FCU}.\overline{FCR}.\overline{FDS}.\overline{ECU}.\overline{ECR}.EDT$	No
	Act	1	1	1	1	1	1		

*Exp = Expected Results, Act = actual results

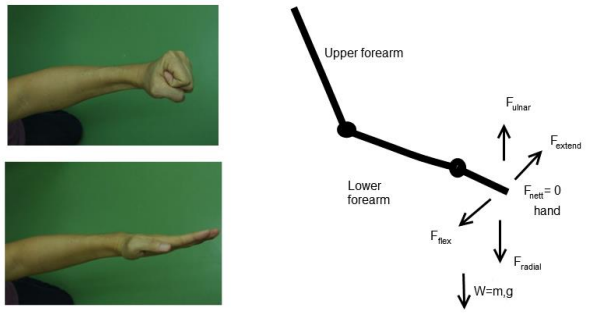

Figure 18 Free body diagram of forces acting unto hand during hand open and close. Insert: photograph of hand close (top) and hand open (bottom)

4.0 CONCLUSION

From this study, several conclusions can be drawn. Noises from manufacturing equipment do contribute to noise. However, we have shown that it should not be a concern as the signal amplitude is still significantly higher than the noise.

A practical EMG amplifier and filter stage circuit can be realized with the low-cost JRC4558 op-amp with acceptable results. However, due to the tolerance of the resistors, care must be taken during selection for the INA stage to ensure resistors are closely matched. Mismatched channel gains will compromise the CMRR of the INA. Despite the potentials in terms of performance Vs price of op-amps, the authors would still recommend to use the integrated INA for the preamp stage. The integrated INA has less component count and does not require resistor matching, thus cutting down development time.

As seen in Table 6, the waveforms acquired showed little correlation to the actual muscle functions. In fact a high level of crosstalk was recorded. This reaffirms that electrode placement is highly critical for good sEMG readings. In our experiment, the electrode pads were large and thus the distance between the inverting and non-inverting channel leads were larger than optimal. This is the main reason for the inaccuracies of the reading whereby the channel placed over a certain muscle did not register significant readings while other unrelated channels showed muscle activities. Future works will be directed to the development of a rigid electrode sleeve.

Acknowledgements

The Malaysian Ministry of Education supports this research through the research grant—FRGS/2/2013/SG02/FKP/02/2/F00176.

References

[1] Berzuini, C., Maranzana-Figini, M., and Bernardinelli, L. 1982. "Effective use of EMG parameters in the assessment of neuromuscular diseases," *Int. J. Biomed. Comput.*, 13(6): 481–499

[2] Pease, W. S., Lew, H. L., and Johnson, E. W. 2007 *Johnson's Practical Electromyography.*, 4th ed. Philadelphia: Lippincott Williams & Wilkins,

[3] Cannan J.,and Hu, H. 2013. "Automatic user identification by using forearm biometrics," in *2013 IEEE/ASME International Conference on Advanced Intelligent Mechatronics*. 710–715.

[4] Jamaluddin, F. N., Ahmad, S. A., Noor, S. B. M., and Hassan, W. Z. W. 2014. "Future direction of the electromyography based method to evaluate muscle fatigue," in *2014 4th*

International Conference on Engineering Technology and Technopreneuship (ICE2T). 314–319.

[5] Artemiadis, P. 2012. "EMG-based Robot Control Interfaces: Past, Present and Future," in *Advances in Robotics & Automation*. 01(02): 10–12.

[6] Zhou, Z. 2010. *Manufacturing Intelligence for Industrial Engineering: Methods for System Self-Organization, Learning, and Adaptation: Methods for System Self-Organization, Learning, and Adaptation*. IGI Global

[7] Oborski, P. "2004. Man-machine interactions in advanced manufacturing systems," *Int. J. Adv. Manuf. Technol.* 23(3–4): 227–232

[8] Hashim, A. Y. B., Maslan, M. N., Izamshah, R. and Mohamad, I. S. 2014. "Delivering key signals to the machine: seeking the electric signal that muscles emanate," *J. Phys. Conf. Ser.* 546: 012020,

[9] Hashim, A. Y. B., Fu, Z., Jamaludin, Z., and Mohamad, I. S. 2015. "How electromyography readings from the human forearm are made cryptic , trivial , or non-trivial information for use in synthetic systems," in *Proceedings of 2015 5th International Conference on Biomedical Engineering and Technology*

[10] Bitzer, S., Hardware, A. E. M. G., and Van Der Smagt, P. 2006. "Learning EMG control of a robotic hand: Towards Active Prostheses," in *Proceedings of the 2006 IEEE International Conference on Robotics and Automation*. May: 2819–2823.

[11] Shenoy, P., Miller, K. J., Crawford, B. and Rao, R. N. 2008."Online electromyographic control of a robotic prosthesis.," *IEEE Trans. Biomed. Eng.* 55(3): 1128–35

[12] Northrop, R. 2001. *Noninvasive Instrumentation and Measurement in Medical Diagnosis*. CRC Press

[13] Artemiadis P., and Kyriakopoulos, K. 2010. "EMG-based control of a robot arm using low-dimensional embeddings," *Robot. IEEE Trans.* 393–398,

[14] Itou, T. and Terao, M. 2001. "Mouse cursor control system using EMG," *23rd Annu. Int. Conf. IEEE Eng. Med. Biol. Soc.* 1368–1369

[15] Castellini, C., Van Der Smagt, P., Sandini, G., and Hirzinger, G. 2008. "Surface EMG for force control of mechanical hands," *2008 IEEE Int. Conf. Robot. Autom.* 725–730

[16] Leijnse, J. N. A. L. 2008.Campbell-Kyureghyan, N. H., Spektor, D., and Quesada, P. M. "Assessment of individual finger muscle activity in the extensor digitorum communis by surface EMG.," *J. Neurophysiol.* 100(6): 3225–35.

[17] Vogel, J., Bayer, J., and Van Der Smagt, P. 2013. "Continuous robot control using surface electromyography of atrophic muscles," *2013 IEEE/RSJ Int. Conf. Intell. Robot. Syst.* 845–850

[18] Stoica, A., Assad, C., Wolf, M., You, K. S., Pavone, M., Huntsberger, T., and Iwashita, Y. 2012. "Using arm and hand gestures to command robots during stealth operations," in *Multisensor, Multisource Information Fusion: Architectures, Algorithms, and Applications 2012*

[19] Tortora, G. J., and Derrickson, B. 2009. *Principles of Anatomy and Physiology*, 12th ed. John Wiley & Sons,

[20] Wang, J., and Bronlund, J. E. 2013. "Surface EMG Signal Amplification and Filtering," *Int. J. Comput. Appl. (0975 – 8887)*, vol. 82, no. November. 15–22

[21] Muhammad Zahak Jamal. 2012. "Signal Acquisition Using Surface EMG and Circuit Design Considerations For Robotic Prosthesis," in *Computational Intelligence in Electromyography Analysis - A Perspective on Current Applications and Future Challenges*, InTech. 427–448.

[22] Shobaki, M. M., Malik, N. A., Khan, S., Nurashikin, A., Haider, S., Larbani, S., Arshad, A., and Tasnim, R. 2013. "High Quality Acquisition of Surface Electromyography – Conditioning Circuit Design," *IOP Conf. Ser. Mater. Sci. Eng.* 53: 012027

[23] Guerreiro, T., Jorge, J., Jo, T., Armando, J., and Jorge, P. 2006. "Emg as a daily wearable interface," in *GRAPP 2006: Proceedings of the First International Conference on Computer Graphics Theory and Applications*

[24] De Luca, C. J. 2002. "Surface Electromyography: Detection and Recording," *DelSys Inc.* 10(2): 1–10,

[25] Moore K. L., and Dalley, A. F. 1999. *Clinically Oriented Anatomy*. Baltimore: Lippincott Williams & Wilkins